BIOLOGICAL SCIENCES: Ecology

A unifying framework for the transient parasite dynamics of migratory hosts

Stephanie J. Peacock[1*], Martin Krkošek[2], Mark A. Lewis[3], Péter K. Molnár[2,4]

1. Department of Biological Sciences
University of Calgary
2500 University Dr NW
Calgary AB T2N 1N4
Canada
ORCID: orcid.org/0000-0001-5016-2153

2. Department of Ecology and Evolutionary Biology
University of Toronto
25 Willcocks St.
Toronto ON M5S 3B2
Canada

3. Departments of Biological Sciences & Mathematical and Statistical Sciences
University of Alberta
Central Academic Building (CAB) 632
Edmonton AB T6G 2G1
Canada

4. Laboratory of Quantitative Global Change Ecology
Department of Biological Sciences
University of Toronto Scarborough
1265 Military Trail
Toronto ON M1C 1A4
Canada
ORCID: orcid.org/0000-0001-7260-2674

*Corresponding author: Stephanie J. Peacock <stephanie.peacock@ucalgary.ca>

Abstract

Migrations allow animals to track seasonal changes in resources, find mates, and avoid harsh climates, but these regular, long-distance movements also have implications for parasite dynamics and animal health. Migratory animals have been dubbed "superspreaders" of infection, but migration can also reduce parasite burdens within host populations via migratory escape from contaminated habitats and transmission hotspots, migratory recovery due to parasite mortality, and migratory culling of infected individuals. Here, we show that a single migratory host-macroparasite model can give rise to these different phenomena under different parameterizations, providing a unifying framework for a mechanistic understanding of the parasite dynamics of migratory animals. Importantly, our model includes the impact of parasite burden on host movement capability during migration, which can lead to "parasite-induced migratory stalling" due to a positive feedback between increasing parasite burdens and reduced movement. Our results provide general insight into the conditions leading to different health outcomes in migratory wildlife. Our approach lays the foundation for tactical models that can help understand, predict, and mitigate future changes of disease risk in migratory wildlife that may arise from shifting migratory patterns, loss of migratory behavior, or climate effects on parasite development, mortality, and transmission.

Keywords: migration, wildlife health, host-parasite, population dynamics

Significance statement

When animals migrate, they take their parasites with them. Or not. Understanding infectious disease in migratory animals is challenging because the vast distances covered result in variable host densities and infection pressure and make it difficult to collect data. Empirical studies show that migrants may have higher, lower, or the same infection intensity as residents. We present a model that produces different infection patterns and migration outcomes under different parameters, laying a theoretical foundation for exploring what may be driving observed diverse patterns in nature. Our model can help guide empirical studies, suggesting when and where data need to be collected in order to distinguish mechanisms, and inform targeted management and conservation efforts.

Introduction

The interactions between animals and their parasites can be profoundly affected by host movement. The mass migrations of entire populations that occur in migratory animals, in particular, can have substantial consequences on parasitism levels and the health of the hosts (1, 2), but the underlying dynamics are complex and difficult to disentangle. Multiple, non-exclusive mechanisms are simultaneously at play – of which some can amplify the impacts of parasitism (3) while others can benefit host health (1, 4). Migrations can compromise host immune systems (5, 6), expose hosts to new pathogens, increase host densities and transmission rates, and spread parasites to uninfected populations (3). Conversely, "migratory escape" from parasitism can occur when hosts move away from habitats where parasites have accumulated, such as breeding and overwintering grounds (7–10). Migratory escape should result in declining parasite burdens with migration so long as the hosts are able to "outrun" their parasites before reinfection occurs, a process that depends both on migration speed of the host and transmission rate of the parasites. The rate of within-host parasite mortality will affect how quickly migratory hosts "recover" from infection after escape (11). Migratory culling (12) and migratory stalling (13) may also reduce mean parasite burdens throughout the migration, but the mechanisms and population outcomes differ from those for migratory escape: the most heavily parasitized individuals, often at the trailing end of the migration, may not complete the migration (stalling) or die trying to do so (culling), thus resulting in smaller, but overall healthier, populations at the end of the migration. The relative impact of migratory

77 culling and stalling will depend on the strength of nonlethal and lethal effects of parasitism on
78 host mortality and movement, respectively.

79 Understanding the parameters that give rise to these different parasite-related outcomes
80 in migratory hosts is essential for predicting and managing wildlife health in the face of climate-
81 associated changes in parasite dynamics (14) and shifting migration patterns (15).
82 Disentangling the different mechanisms is difficult in practice because (i) migratory animals
83 often cover vast distances, making it challenging to obtain appropriate data (16), (ii) different
84 mechanisms can lead to the same observed patterns in parasite burdens towards the end of a
85 migration (9), and (iii) appropriate modelling frameworks for studying spatially dynamic host-
86 parasite interactions have only became available recently (2, 13, 17–19). The development of
87 models and theory to describe the interactions between migratory host and parasite
88 populations is an alternative that can offer deep and generalizable insights into conditions
89 under which we might expect migration to reduce disease risk via escape or culling, or
90 contribute to pathogen spread based on characteristics of the host, parasite, and environment
91 (20). Despite increasing recognition of the diverse effects of host movement on disease
92 dynamics (1) and accumulating empirical examples (9, 10, 21–23), theoretical frameworks for
93 studying disease dynamics during long-distance movement have been lagging (20).

94 Macroparasites (e.g. helminths, arthropods) are key players in the lives of most animals
95 (24) and are ideally suited for investigating the parasite dynamics of migratory animals: (i) most
96 macroparasites have clearly structured life cycles, often with a free-living stage that slows
97 reinfection to hosts; (ii) the parasite burdens of hosts can usually be understood as an
98 emergent property of host and parasite traits, such as the length of the free-living stage and the

movement speed of hosts (13); and (iii) host performance (22), including survival, movement speed (12), endurance (25), and stamina (26), tends to decline with increasing parasite burden, which represents the intensity of infection. The interactions of migratory animals with their macroparasites have, however, largely been neglected in the literature to date, with most existing models focusing on individual-based or metapopulation models for microparasites (20). In these existing models, susceptible and infected hosts are tracked without consideration of parasite burdens (e.g., 2, 17–19). Moreover, most models do not explicitly incorporate the movement of animals during migrations, and those that do (i.e., 2) do not consider how parasite burdens and resultant impacts on host survival and movement may vary among individuals within a population.

Host-macroparasite models that consider parasite burdens of migratory animals are more complex than susceptible-infected models because parasite burdens may vary dynamically in both space, even within a migrating population, and time, within individuals and populations. For example, animals at the trailing edge of the migration may be more parasitized than those at the leading edge because followers are exposed to parasites shed by the leaders. This pattern of higher parasite burdens in late migrators has been observed in several species of migratory birds (27, 28), and may be exacerbated if healthy individuals tend to depart earlier and/or parasitism has negative effects on the movement capacity of hosts. The pattern of infection intensity within a host population can affect the host-parasite dynamics and be informative of the mechanisms (e.g., migratory escape or culling) at play.

To better understand the diversity of mechanisms by which parasitism and host movement interact to affect host health, we refined a recently developed partial-differential-equation

(PDE) model of spatiotemporal host-macroparasite dynamics (13; Fig. 1) to explore conditions under which we might expect migratory escape, migratory culling, and migratory stalling to occur. Unlike previous modelling studies, our approach considers environmentally transmitted macroparasites and how the number of parasites per host (i.e., parasite burden) affects mortality and transmission rates of parasites as well as host movement and survival. We show that the same model can give rise to migratory escape, culling, or stalling depending on the parameterization, providing the first unifying framework for migratory host and macroparasite dynamics. Our model and results are strategic, providing general insight, but could be adapted and made tactical, for example to address questions regarding the impact of changing parameters on specific host-parasite systems.

Results

We employed variants of a spatial host-parasite model (13) to identify conditions under which wildlife populations are likely to experience migratory escape, migratory culling, or migratory stalling. The base model (Fig. 1; black) considers a migratory host population, $\widehat{H}(x,t)$, moving along a one-dimensional migration corridor at a constant speed, *c*. The parasite burden of migrating hosts, $\widehat{P}(x,t)$, decreases as parasites die at per capita rate μ_P, and increases as hosts take up stationary free-living parasite larvae from the environment, *L(x,t)*, at rate β. Infected hosts produce larvae at per-parasite rate λ, and larvae die at per capita rate μ_L. We added complexity to this model in two ways: first, we considered parasite-induced host mortality at per-parasite rate α to understand the dynamics of migratory culling (Fig. 1; blue). Second, we considered the possibility for migrating hosts to stop moving at per-

parasite rate θ to understand the dynamics of migratory stalling (Fig. 1; pink). Higher values of α and θ reflect a greater impact of parasitism on host survival and movement, respectively, which may relate to the strenuousness of the migration and thus susceptibility of the host and/or virulence of the parasite.

The model focuses on host-parasite dynamics during migration and ignores host birth, which occurs during a non-migratory breeding season for many species. In the absence of host birth, non-zero equilibria for parasite burdens and larvae do not exist (29) regardless of the migration speed of hosts (c), transmission rate of parasites (β), mortality rate of parasites (μ_P), or host mortality due to parasitism (α) (see SI appendix for model equations and analysis). However, the time it takes to reach the parasite-free equilibrium and peak parasite burdens *will* depend on these parameters, and these transient dynamics may be more relevant for host populations that have a limited migration duration. We considered the transient dynamics over a 365-day migration period, although this timeframe is arbitrary and does not affect the results (i.e. the parameters can be rescaled to any timeframe to produce the same results).

Simulations generally show initial increases in parasite burdens at the location of peak host density (Fig. 2A; day 1). As the host population migrates, parasite burdens decline at the leading edge of the migrating host population but increase for hosts at the trailing end of the migrating host population, such that the spatial distribution of parasite burdens within the migrating host population forms a slowly varying travelling wave (Fig. 2A; day 80). The front of this wave gradually shifts backwards within the host population as individuals at the leading edge are not exposed to new infections. Eventually, the parasite burden at the trailing edge will also decline (Fig. 2A; day 360). We summarized these dynamics using three metrics: (1) the

time until mean parasite burdens peaked, $t(\bar{P}_{\max})$, (2) the time until parasite burdens declined to initial levels, $t(\bar{P}_0)$, and (3) the peak mean parasite burden among migrating hosts, $\bar{P}_{\max}$ (Fig. 2B). These three metrics are all positively related (it will take longer to reach a higher peak mean parasite burden) but have different practical implications and thus we discuss them all. For models that included host mortality or stopping, we also included the fraction of hosts that were alive and migrating at the time when parasite burdens have declined again to the initial conditions, $\hat{f}(t(\bar{P}_0)) = \sum \hat{H}\big(x, t(\bar{P}_0)\big) / \sum \{\hat{H}\big(x, t(\bar{P}_0)\big) + H\big(x, t(\bar{P}_0)\big)\}$.

Migratory escape

Under the basic model, it took longer to reach peak parasite burdens when the transmission rate was high, migration speed was low, and/or within-host parasite mortality was low (Fig. 3A). At low parasite mortality (μ_P = 0.001 d^{-1} in our simulations), migratory escape was impossible within a year for all but the lowest transmission rates (β = 0.0001 d^{-1}; Fig. 3A-B). At high parasite mortality (μ_P = 0.05 d^{-1}), parasite burdens began to decline within 10 days (Fig. 3A) and declined below initial burdens within 54 days (Fig. 3B) for all values of transmission rate and migration speed that we investigated. Lower migration speeds and/or faster transmission rates also led to higher peak mean parasite burdens (Fig. 3C).

Migratory culling

The addition of parasite-induced host mortality (α) to the model greatly reduced the migration time required for parasite burdens to decline and resulted in much lower peak parasite burdens among migrating hosts. The number of days until parasite burdens declined or reached initial values was more sensitive to changes in α than to changes in β (Fig. 4A,C),

except at very low transmission rates. At low rates of parasite-induced host mortality, the time needed to escape increased with increasing transmission rates up to β = 0.01 d^{-1}, consistent with the general pattern of higher transmission leading to higher parasite burdens and thus longer times to escape. However, as transmission rates increased from β = 0.01 d^{-1} to 0.05 d^{-1}, it took less time for parasite burdens to decline to initial levels (Fig. 4C) because relatively high parasite burdens (Fig. 4E) accelerated the mortality of heavily parasitized hosts (Fig. 4G). The proportion of hosts alive at any given point in time decreased with increasing parasite-induced mortality (Fig. S2B-G). However, because parasite burdens declined to initial faster under high parasite-induced mortality (Fig. 4C), the proportion of hosts alive (i.e., migrating) at that time actually increased with increasing parasite-induced mortality at moderate to high transmission rates (Fig. 4G).

Migratory stalling

When we incorporated parasite-induced stopping of migrating hosts (θ), the time until parasite burdens declined was also reduced, as with parasite-induced mortality (Fig. 4B,D). However, even at low values of θ, a small fraction of hosts was still migrating when their parasite burdens declined below initial values (Fig. 4H) when compared to the fraction still migrating (i.e., still alive) under the migratory culling scenario (Fig. 4G). At the same θ, a larger fraction of the host population ceased migrating as β increased because the peak mean parasite burden was higher (Fig. 5). For hosts that stopped migrating, parasite burdens increased through the 365-day simulation for all but the lowest values of β (Fig. 5A).

Discussion

Multiple simultaneously acting mechanisms make it difficult to unravel the host-parasite dynamics of migrating wildlife. Empirical examples exist for migrants with higher (23, 30, 31), lower (9, 10, 16), and similar (32) parasite burdens as resident hosts, and our analyses suggest that such seemingly idiosyncratic patterns could in fact reflect systematic variation of how key parameters determining the host-parasite dynamics balance against one another. In this paper, we presented a unifying modelling framework for describing the multiple mechanisms by which migration can affect macroparasite transmission and vice versa. Our framework includes, for the first time, the spatial infection dynamics during migration and the impact of infection intensity on host survival and movement. This allowed us to show that migratory escape, culling, and stalling may all be different sides of the same coin, arising from the same model depending on characteristics of the host, the parasite, and the environment.

We have shown that, in theory, complete migratory escape from parasites (i.e., zero parasite burden for all hosts) will always occur if a migrating population traverses uninfested habitats for a long-enough time, because the leading individuals will not be exposed to new infections. With non-zero parasite mortality, these leading individuals will lose their infections and cease to shed parasites to infect the individuals behind. Thus, the parasite front will gradually shift backwards in the host population until all hosts are parasite free. In mathematical terms, the long-term equilibrium of our model is unequivocally a mean parasite burden of zero. In nomadic species or those with long and variable migration routes, complete escape as such may indeed occur (although nomadic animals are more likely to encounter a diversity of parasites and thus may have higher parasite richness due to “environmental

sampling" (4, 23)). However, our simulations suggest that for many species that undergo seasonal migration, complete escape from parasites would likely take much longer than the duration of migration. For seasonal migrants, it is more relevant to consider the transient dynamics over the course of the migration, such as the peak parasite burden and the time that it takes for parasite burdens to drop below the initial level (i.e., the "time to escape"). Our simulations showed that both these metrics increase with increasing parasite transmission rate but decrease with faster migration speeds and increasing parasite mortality rates. In practical terms, this means it is more difficult for hosts to outrun parasites that have long-lived adult parasite stages within the host and short environmental transmission stages relative to the time it takes for trailing individuals to pass larvae laid down by the leading individuals of a host population (which in turn is determined by the movement speed and spatial spread of the hosts).

Perhaps counterintuitively, migratory escape becomes easier for the host population when high parasite burdens are lethal or have sublethal effects on host movement. When heavily parasitized hosts cease to migrate (either due to stalling or death), their parasites are also removed from the migrating host population, thus reducing transmission and reinfection. As such, both migratory culling and migratory stalling can improve overall host population health, but this comes at the expense of smaller and/or more fragmented populations. For individual hosts that are left behind, separation from the migratory group may undermine other benefits of group living, increasing the susceptibility of hosts to other forms of mortality such as predation (33) and decreasing the benefits that migration itself conferred such as mating opportunities and favorable environmental conditions for growth and reproduction. Whether

249 or not culling and stalling benefit the host population as a whole thus depends on the strengths
250 of these processes (i.e., the magnitude of parameters for parasite-induced mortality and
251 stalling), as well as on whether host numbers and cohesive populations are more valuable than
252 overall population health (which may, for example, be the case for long-lived species with slow
253 population growth rates). Indeed, if the impact of parasites on movement capacity is high
254 enough, strong feedback loops between parasitism-induced slow movement and increased
255 parasite exposure due to slow movement, can result in entire host populations stalling in
256 infection hotspots, with cascading implications for both host population health and ecosystems
257 missing the migrants.

258 The potential for parasite-induced migratory stalling may be greatest among species that
259 rely on group cohesion for foraging benefits, predator evasion, or navigational accuracy during
260 long-distance migrations (34). For one, group cohesion may increase host and parasite
261 densities, and thus infection rates, leading to higher parasite burdens. Stalling may occur
262 abruptly if healthy individuals choose to maintain group cohesion with infected hosts that have
263 reduced migratory ability in order to reap the benefits of group living. In such cases, there may
264 be a threshold prevalence of infection within the host population, above which stalling would
265 be expected due to the strong behavioral tendency to maintain the flock, herd, or school.
266 Alternately, healthy individuals may avoid contact with parasitized conspecifics (7), in which
267 case fragmentation of the host population may occur at lower parasite burdens than we would
268 expect based on declining movement rates alone. Such avoidance behavior may therefore
269 accelerate migratory stalling, to the benefit of those hosts that escape. The current model does
270 not consider individual movement decisions that may lead to this type of collective behavior,

271 but future research might consider individual-based models in which movement decisions are
272 based on both conspecific distance (35) and parasite burden.

273 Our analyses indicate that distinguishing between escape, stalling and culling may not be
274 possible given data from the beginning and end of a migration only, as all mechanisms suggest
275 a declining parasite burden once the peak has been passed. Distinguishing between stalling
276 and culling may be particularly difficult because both mechanisms result in fewer and healthier
277 hosts reaching their destination. Nevertheless, such distinctions can be important because the
278 slowing of movement without actual parasite-induced mortality may have very different
279 consequences for the conservation of host populations, as well as for the persistence of
280 parasites, than parasite-induced culling. Migratory stalling could potentially lead to non-
281 migratory sub-populations that persist through time, and there are examples of ungulate
282 species that undergo partial migration for which the sedentary groups experience higher
283 parasite burdens than the migratory groups (36, 37). Our framework suggests that in order to
284 distinguish between the various mechanisms affecting migratory host-parasite dynamics, it
285 would be critical to collect data along the migration route, including on host densities, host
286 spread, and parasite burdens (this may be easier for terrestrial migrants than, for example,
287 birds). Linking such data with model predictions for the shifting travelling wave of parasite
288 burdens during a migration, in particular, could help estimate key model parameters and
289 driving mechanisms.

290 Our models are strategic rather than tactical: intending to illuminate general mechanisms
291 rather than describing any system specifically. Species-specific parameters and additional
292 population dynamics mechanisms are, however, easily incorporated. Adaptations of the model

could, for example, be used to explore the role of age-structure in migratory host-parasite dynamics (e.g., newborn caribou calves having lower movement speeds but also leaving the breeding grounds with relatively low parasite burdens, 8, 14), the role of differing migration strategies (e.g. circular migrations reducing reinfection risks compared to migration routes that are simply reversed seasonally), the role of population dynamics processes that usually occur between migrations (e.g., births), as well as different parasite life cycles and infection strategies (e.g., a requirement of an intermediate host for larval development slowing reinfection and facilitating escape). We have only considered a single host – single parasite system, but the model could be expanded to include multiple parasites, multiple host populations, and/or generalist parasites, allowing for investigations into how migration may affect parasite diversity as well as intensity (4, 23). We also call for the development of microparasite models that explicitly capture the dynamics throughout the migratory period (or transient phase, as described in (2)) and impacts of the parasites during the migration, but suspect that similar results would be obtained in that case, albeit for slightly different reasons. For example, we modelled parasite transmission via a free-living larval stage, whereas for many microparasites the direct contact between susceptible and infected individuals is necessary. This could be approximated via an infinitely short free-living stage in our system, or directly modelled in an SIR framework. Either way, we suspect that lagging infection waves, with low and high infections at the leading and trailing ends, respectively, would also arise, but now because of the reduced chance of encountering an infected conspecific at the lower-density, leading end of a migration.

Conclusions

Wildlife migrations have been on the decline (15, 38) due to a number of factors including anthropogenic resource subsidies that encourage sedentary life-histories (e.g., milkweed planting for butterflies (39)) and industrial developments that directly impede migratory pathways (e.g., the building of hydroelectric dams on major salmon-bearing rivers in the US in the 1960s (40)). The loss of migratory behavior may have dramatic consequences for the transmission of parasitic diseases among wildlife, but disentangling the interactions between migration and parasitism has been hindered by the lack of a unifying framework to describe the diverse outcomes observed in nature (1). We have presented a spatial model for migratory host-macroparasite dynamics that incorporates the impact of parasite burdens on host mortality and migratory capabilities and can describe the mechanisms that lead to parasite spread, migratory escape, migratory culling, or migratory stalling. These general insights may help guide empirical studies to differentiate the potential health outcomes for migratory wildlife, and help understand how parasitic diseases will change in the Anthropocene when migration patterns are changing (15), emerging infectious diseases are on the rise (41, 42), and climate change is altering host-parasite dynamics (43, 44).

Materials and methods

Model

We refined a previously described model of migratory host-macroparasite dynamics (13) to focus on the mechanisms of migratory escape, migratory culling, and migratory stalling. The model consists of seven coupled partial differential equations (see SI appendix for equations)

335 that track spatial and temporal changes in the density of moving and stationary host
336 populations, the mean parasite burdens of both moving and stationary hosts, the variance-to-
337 mean ratios of the distribution of parasites among both stationary and moving hosts, and the
338 density of stationary parasite larvae in the environment (Fig. 1). Unlike most host-
339 macroparasite models, we modelled the variance-to-mean ratios as dynamic variables because
340 host processes that affect the mean parasite burden (e.g., parasite-induced mortality and
341 parasite-mediated movement capacity) can also affect the spatial distribution of parasites
342 among hosts (29). This is particularly important when considering migratory hosts because
343 spatial variability in the aggregation of parasites can interact with host movement to affect
344 host-parasite dynamics (13).

345 Parasites were distributed among hosts according to the negative binomial, consistent
346 with previous models and empirical data (45). We ignored host birth and natural host mortality
347 in order to focus on the parasite-mediated processes during migration.

348 We numerically simulated the system of equations on a discrete space-time grid. The
349 time step was adjusted depending on migration speed in the simulation so that $\delta t = \eta\ \delta x/c$,
350 where η is a whole number and c is the speed of moving hosts. At each time step, we first
351 applied host movement and then applied parasite-induced host mortality, parasite attachment,
352 parasite mortality, and host stopping, using the operator-splitting method (46). We assumed
353 Neumann boundary conditions where the derivative across the boundary is zero.

354 We began all simulations with a Gaussian spatial distribution of migrating hosts
355 centered at x =0 km with the same parasite burden through space (Fig. S1). The initial
356 distribution of stationary parasite larvae in the environment mirrored the distribution of hosts,

with a peak density of 10 times the peak host density to represent the build-up of parasite larvae in overwintering or breeding habitats prior to migration. For the migratory stalling case, we started with a small fraction of stationary hosts at all points in space to avoid numerical problems because the stationary host density appears in the denominator within model equations. These stationary hosts had the same, constant parasite burdens as their migratory counterparts. Further details on the model can be found in the SI appendix and R code to reproduce simulations is available at https://github.com/sjpeacock/Parasit-mig-patterns.

Acknowledgements

Funding for this study came from the Natural Sciences and Engineering Research Council of Canada (NSERC): Postdoctoral Fellowship to SJP, Discovery grants to MAL, MK, and PKM, and Canada Research Chairs to MAL and MK. PKM is also grateful for funding from the Canada Foundation for Innovation (CFI) John R. Evans Leaders Fund and the Ministry of Research, Innovation and Sciences (MRIS) Ontario Research Fund.

References

1. Altizer S, Bartel R, Han BA (2011) Animal Migration and Infectious Disease Risk. *Science (80-)* 331(6015):296–302.
2. Daversa DR, Fenton A, Dell AI, Garner TWJ, Manica A (2017) Infections on the move: how transient phases of host movement influence disease spread. *Proc R Soc B Biol Sci* 284(1869):20171807.
3. Fritzsche McKay A, Hoye BJ (2016) Are Migratory Animals Superspreaders of Infection? *Integr Comp Biol* 56(2):260–267.
4. Shaw AK, Sherman J, Barker FK, Zuk M, Shaw AK (2018) Metrics matter: the effect of parasite richness, intensity and prevalence on the evolution of host migration. *Proc R Soc B Biol Sci* 285:20182147.
5. Lisovski S, et al. (2018) The roles of migratory and resident birds in local avian influenza infection dynamics. *J Appl Ecol* 55(6):2963–2975.
6. van Dijk JGB, Matson KD (2016) Ecological Immunology through the Lens of Exercise Immunology: New Perspective on the Links between Physical Activity and Immune Function and Disease Susceptibility in Wild Animals. *Integr Comp Biol* 56(2):icw045.
7. Loehle C (1995) Social Barriers to Pathogen Transmission in Wild Animal Populations. *Ecology* 76(2):326–335.
8. Folstad I, Nilssen AC, Halvorsen O, Andersen J (1991) Parasite avoidance: the cause of post-calving migrations in Rangifer? *Can J Zool* 69:2423–2429.
9. Bartel RA, Oberhauser KS, De Roode JC, Altizer SM (2011) Monarch butterfly migration

391 and parasite transmission in eastern North America. *Ecology* 92(2):342–351.
392 10. Poulin R, et al. (2012) Migration as an escape from parasitism in New Zealand galaxiid
393 fishes. *Oecologia* 169:955–963.
394 11. Shaw AK, Binning SA (2016) Migratory Recovery from Infection as a Selective Pressure for
395 the Evolution of Migration. *Am Nat* 187(4):491–501.
396 12. Bradley CA, Altizer S (2005) Parasites hinder monarch butterfly flight: implications for
397 disease spread in migratory hosts. *Ecol Lett* 8:290–300.
398 13. Peacock SJ, Bouhours J, Lewis MA, Molnár PK (2018) Macroparasite dynamics of
399 migratory host populations. *Theor Popul Biol* 120:29–41.
400 14. Dobson A, Molnár PK, Kutz S (2015) Climate change and Arctic parasites. *Trends Parasitol*
401 31(5):181–188.
402 15. Wilcove DS, Wikelski M (2008) Going, going, gone: Is animal migration disappearing?
403 *PLoS Biol* 6(7):1361–1364.
404 16. Mijele D, et al. (2016) Influence of Massive and Long Distance Migration on Parasite
405 Epidemiology : Lessons from the Great Wildebeest Migration. *Ecohealth* 13(4):708–719.
406 17. Hall RJ, Altizer S, Bartel RA (2014) Greater migratory propensity in hosts lowers pathogen
407 transmission and impacts. *J Anim Ecol* 83:1068–1077.
408 18. Hall RJ, Brown LM, Altizer S (2016) Modeling vector-borne disease risk in migratory
409 animals under climate change. *Integr Comp Biol* 56(2):icw049.
410 19. Johns S, Shaw AK (2015) Theoretical insight into three disease-related benefits of
411 migration. *Popul Ecol* 58:213.
412 20. White LA, Forester JD, Craft ME (2018) Dynamic, spatial models of parasite transmission

413 in wildlife: Their structure, applications and remaining challenges. *J Anim Ecol* 87:559–
414 580.
415 21. Lecce I Di, et al. (2018) Patterns of Midichloria infection in avian-borne African ticks and
416 their trans-Saharan migratory hosts. *Parasit Vectors* 11:106.
417 22. Risely A, Klaassen M (2018) Migratory animals feel the cost of getting sick : A meta-
418 analysis across species. *J Anim Ecol* 87:301–314.
419 23. Teitelbaum CS, Huang S, Hall RJ, Altizer S (2018) Migratory behaviour predicts greater
420 parasite diversity in ungulates. *Proc R Soc B Biol Sci* 285:20180089.
421 24. Dobson A, Lafferty KD, Kuris AM, Hechinger RF, Jetz W (2008) Homage to linnaeus: How
422 many parasites? How many hosts? *Proc Natl Acad Sci* 105:11482–11489.
423 25. Mages PA, Dill LM (2010) The effect of sea lice (*Lepeophtheirus salmonis*) on juvenile pink
424 salmon (*Oncorhynchus gorbuscha*) swimming endurance. *Can J Fish Aquat Sci*
425 67(12):2045–2051.
426 26. Kocan R, LaPatra S, Gregg J, Winton J, Hershberger P (2006) Ichthyophonus-induced
427 cardiac damage: A mechanism for reduced swimming stamina in salmonids. *J Fish Dis*
428 29(9):521–527.
429 27. DeGroote LW, Rodewald PG (2010) Blood parasites in migrating wood-warblers
430 (Parulidae): Effects on refueling, energetic condition, and migration timing. *J Avian Biol*
431 41(2):147–153.
432 28. Møller AP, de Lope F, Saino N (2004) Parasitism, Immunity, and Arrival Date in a
433 Migratory Bird, the Barn Swallow. *Ecology* 85(1):206–219.
434 29. Adler FR, Kretzschmar M (1992) Aggregation and stability in parasite-host models.

435 *Parasitology* 104:199–205.
436 30. Hasselquist D, Östman Ö, Waldenström J, Bensch S (2007) Temporal patterns of
437 occurrence and transmission of the blood parasite *Haemoproteus payevskyi* in the great
438 reed warbler *Acrocephalus arundinaceus*. *J Ornithol* 148(4):401–409.
439 31. Gylfe Å, Bergström S, Lundström J, Olsen B (2000) Reactivation of Borrelia infection in
440 birds. *Nature* 403:724–725.
441 32. Carbó-Ramírez P, Zuria I (2015) Immune condition and blood parasites in three sparrow
442 species with different migratory status in central Mexico. *Avian Biol Res* 8(3):167–174.
443 33. Evans JC, Votier SC, Dall SRX (2016) Information use in colonial living. *Biol Rev* 91(3):658–
444 672.
445 34. Beauchamp G (2011) Long-distance migrating species of birds travel in larger groups. *Biol*
446 *Lett* 7(5):692–694.
447 35. Couzin ID, Krause J, James R, Ruxton GD, Franks NR (2002) Collective memory and spatial
448 sorting in animal groups. *J Theor Biol* 218(1):1–11.
449 36. Pruvot M, et al. (2016) Better Alone or in Ill Company? The Effect of Migration and Inter-
450 Species Comingling on *Fascioloides magna* Infection in Elk. *PLoS One* 11(7):e0159319.
451 37. Mysterud A, Qviller L, Meisingset EL, Viljugrein H (2016) Parasite load and seasonal
452 migration in red deer. *Oecologia* 180(2):401–407.
453 38. Berger J (2004) The last mile: How to sustain long-distance migration in mammals.
454 *Conserv Biol* 18(2):320–331.
455 39. Satterfield DA, Maerz JC, Altizer S (2015) Loss of migratory behaviour increases infection
456 risk for a butterfly host. *Proc R Soc B Biol Sci* 282:20141734.

40. Marschall EA, Mather ME, Parrish DL, Allison GW, McMenemy JR (2011) Migration delays caused by anthropogenic barriers: modeling dams, temperature, and success of migrating salmon smolts. *Ecol Appl* 21(8):3014–3031.

41. Jones KE, et al. (2008) Global trends in emerging infectious diseases. *Nature* 451(7181):990–993.

42. Cunningham AA, Daszak P, Wood JLN (2017) One Health, emerging infectious diseases and wildlife: two decades of progress ? *Philos Trans R Soc B* 372:20160167.

43. Harvell CD, et al. (2002) Climate Warming and Disease Risks for Terrestrial and Marine Biota. *Science (80-)* 296(5576):2158–2162.

44. Molnár PK, Kutz SJ, Hoar BM, Dobson AP (2013) Metabolic approaches to understanding climate change impacts on seasonal host-macroparasite dynamics. *Ecol Lett* 16:9–21.

45. Shaw DJ, Grenfell BT, Dobson AP (1998) Patterns of macroparasite aggregation in wildlife host populations. *Parasitology* 117:597–610.

46. Hundsdorfer W, Verwer JG (2003) *Numerical solution of time-dependent advection-diffusion-reaction equations* (Springer-Verlag Berlin Heidelberg) doi:10.1007/978-3-662-09017-6.

Figure Legends

Fig. 1. Schematic of the model used to describe the host-parasite dynamics of migratory wildlife. State variables include the host density $H(x,t)$, mean parasite burden $P(x,t)$ and density of stationary parasite larvae $L(x,t)$, with the hat denoting migrating hosts and their parasites. The basic model ignores host mortality and stopping but includes host movement at speed c (black arrows and grey boxes), and allowed us to focus on migratory escape and recovery from parasitism. We added complexity to this basic model in two ways: (1) including parasite-induced host mortality at per-parasite rate α (blue arrow), to capture the dynamics of migratory culling, and (2) including stationary hosts and parasite-induced stopping at per-parasite rate θ (pink), which led to parasite-induced migratory stalling. Description of other parameters and base values are in Table 1. Model equations are given in the SI appendix.

Fig. 2. A) A simulation of migratory escape using the basic model (Fig. 1), where the host population (grey line) is initially Gaussian distributed around $x = 0$ at $t = 0$ days and migrates at $c = 50$ km d^{-1}. The parasite burden (black line) is initially $P(x,t_0) = 5$ parasites $host^{-1}$ (horizontal dotted line). The mean parasite burden across all migrating hosts, P, is the convolution of the parasite burden (black line) and the host density (normalized to integrate to one). B) The mean parasite burden initially increased but then declined with increasing duration of migration. We capture these dynamics using three metrics: (1) the time to peak mean parasite burden, $t(P_{max})$ (vertical blue line), (2) time until parasite burdens declined to initial, $t(P_0)$ (vertical purple line), and the peak mean parasite burden,

494 P_{max} (horizontal pink line). Other parameters in this simulation were: $\lambda = 0.03\ d^{-1}$, $\mu_L =$
495 $0.015\ d^{-1}$, $\mu_P = 0.01\ d^{-1}$, and $\beta = 0.004\ d^{-1}$.

496 Fig. 3. The transient dynamics under the base model and "escape" parameterization (Table 1)
497 over a 365-day period, summarized as the days until peak parasite burdens (blue), the
498 days until parasite burdens decline to initial (purple), and the peak mean parasite burden
499 (pink; Fig. 2). Each metric is shown over increasing migration speed of hosts (x-axis),
500 transmission rate of parasites (y-axis), and mortality rate of parasites (panels, left to
501 right). The asterisk indicates parameter values for the simulation shown in Fig. 2.

502 Fig. 4. Transient dynamics of the model over a 365-day period with parasite transmission rates
503 from $\beta = 0$ to $0.05\ d^{-1}$ (y-axis) and per-parasite rates of host mortality from $\alpha = 0$ to 0.003
504 d^{-1} (x-axis) in the "migratory culling" scenario (left) or per-parasite rates of host stopping
505 from $\theta = 0$ to $0.004\ d^{-1}$ in the "migratory stalling" scenario (right). Dynamics are
506 summarized as the days until peak parasite burdens (A-B, blue), the days until parasite
507 burdens decline to initial (C-D, purple), the peak mean parasite burden (E-F, pink), and the
508 fraction of hosts alive and migrating at the time when parasite burdens have declined to
509 initial (G-H, yellow). Black regions in G, H are parameter combinations for which the
510 fraction of hosts migrating at $t(\bar{P}_0)$ could not be calculated as parasite burdens did not
511 reach $\bar{P}_0$ within the 365-day simulation (C,D). Host-parasite dynamics over the 365-day
512 migration are shown in Fig. 5 for parameter combinations indicated by open points in the
513 stalling panels (B, D, F, H).

514 Fig. 5. (A-C) The mean parasite burden of migrating (solid black lines) and stationary hosts
515 (dotted grey lines) over a 365-day simulation for three different combinations of parasite-

induced stopping (θ) and transmission rate (β) (Fig. 4, right): (1) no stopping and high transmission (circle), (2) stopping and high transmission (up triangle), (3) stopping and low transmission (down triangle). Other parameters are at the "stalling" values in Table 1. (D-F) The corresponding fraction of hosts that are migrating (solid black lines) and stationary (dotted grey lines).

Tables

Table 1. Base parameter values used in simulations of the host-parasite model (Fig. 1; see SI appendix for equations). The parameter ranges explored when considering escape, culling, and stalling are shown in bold.

Symbol	Description	Value in simulations		
		Escape/ Recovery	**Culling**	**Stalling**
λ	Parasite production (d^{-1})	0.03	0.03	0.03
μ_L	Free-living parasite larvae death (d^{-1})	0.015	0.015	0.015
β	Uptake of parasite larvae by hosts (d^{-1})	**0.0001 – 0.022**	**0.0001 – 0.05**	**0.0001 – 0.05**
c	Speed of migrating hosts (km d^{-1})	**1 – 100**	25	25
μ_P	Within-host parasite natural death (d^{-1})	**0.001 – 0.05**	0.01	0.01
α	Parasite-induced host death (d^{-1})	0	**0 – 0.003**	0
θ	Per-parasite increase in stopping (d^{-1})	0	0	**0 – 0.004**

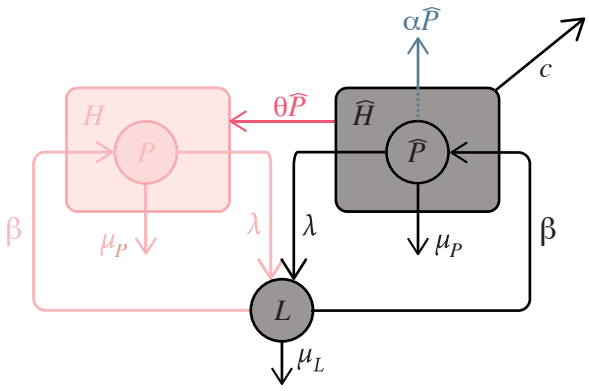
$\alpha\widehat{P}$
c
$\theta\widehat{P}$
H
P
$\widehat{H}$
$\widehat{P}$
β
μ_P
λ
λ
μ_P
β
L
μ_L

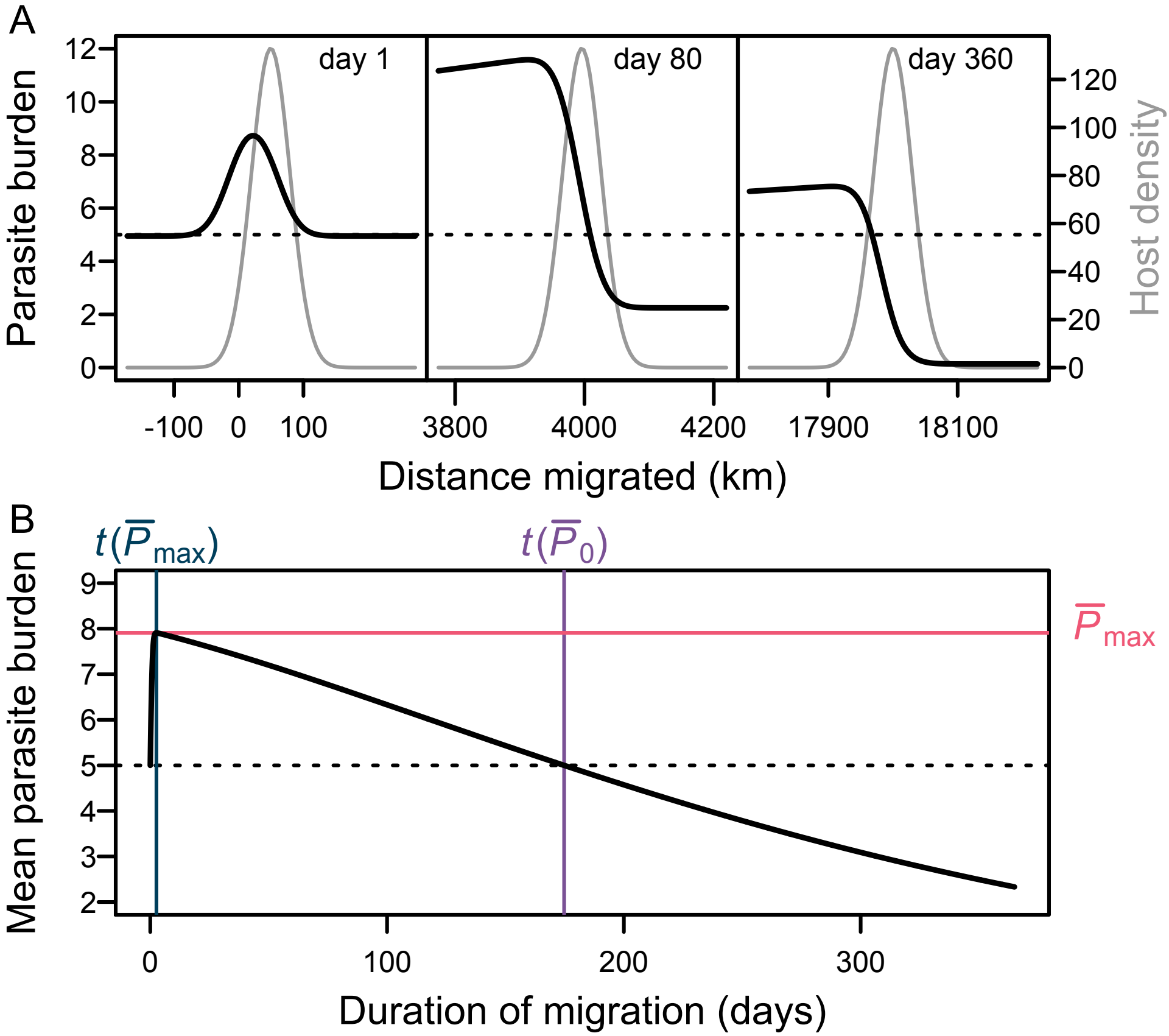
A
Parasite burden
Host density
day 1
day 80
day 360
0
2
4
6
8
10
12
0
20
40
60
80
100
120
-100
0
100
3800
4000
4200
17900
18100
Distance migrated (km)
B
Mean parasite burden
$t(\overline{P}_{max})$
$t(\overline{P}_0)$
$\overline{P}_{max}$
2
3
4
5
6
7
8
9
0
100
200
300
Duration of migration (days)

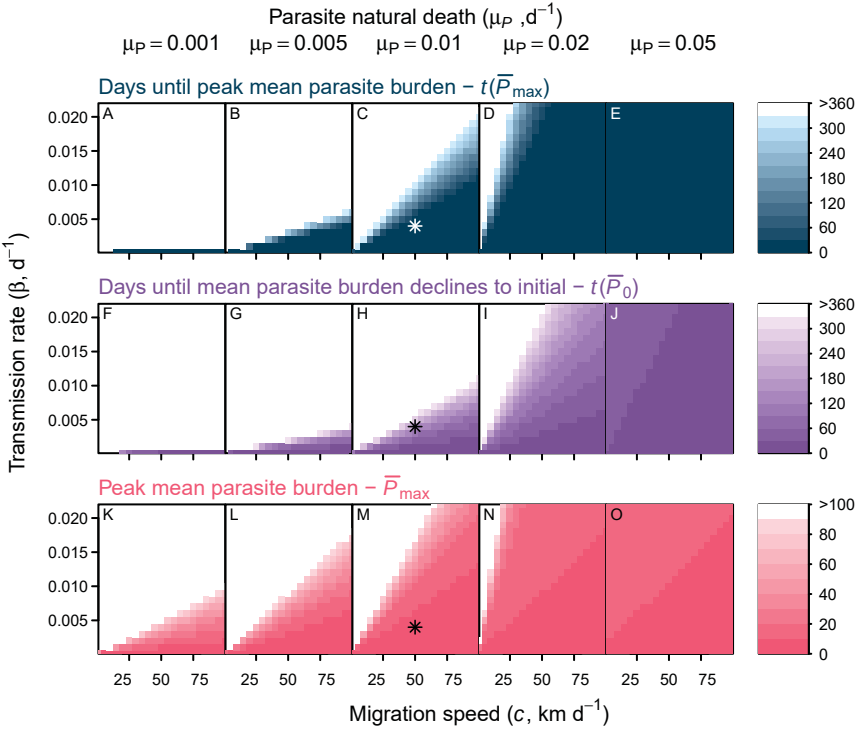
Parasite natural death (μ_P ,d^{-1})
$\mu_P = 0.001$
$\mu_P = 0.005$
$\mu_P = 0.01$
$\mu_P = 0.02$
$\mu_P = 0.05$
Days until peak mean parasite burden − $t(\overline{P}_{max})$
Days until mean parasite burden declines to initial − $t(\overline{P}_0)$
Peak mean parasite burden − $\overline{P}_{max}$
A
B
C
D
E
F
G
H
I
J
K
L
M
N
O
0.020
0.015
0.010
0.005
>360
300
240
180
120
60
0
>100
80
60
40
20
0
25
50
75
Transmission rate (β, d^{-1})
Migration speed (c, km d^{-1})

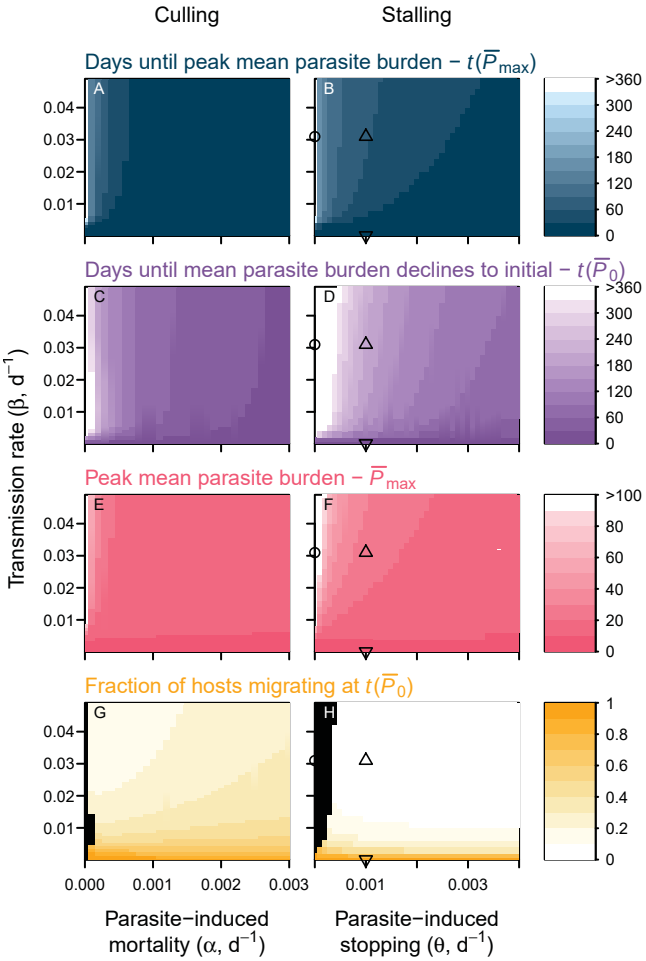
Culling
Stalling
Days until peak mean parasite burden − $t(\overline{P}_{max})$
Days until mean parasite burden declines to initial − $t(\overline{P}_0)$
Peak mean parasite burden − $\overline{P}_{max}$
Fraction of hosts migrating at $t(\overline{P}_0)$
A
B
C
D
E
F
G
H
Transmission rate (β, d^{-1})
0.04
0.03
0.02
0.01
>360
300
240
180
120
60
0
>100
80
40
20
1
0.8
0.6
0.4
0.2
0.000
0.001
0.002
0.003
Parasite−induced mortality (α, d^{-1})
Parasite−induced stopping (θ, d^{-1})

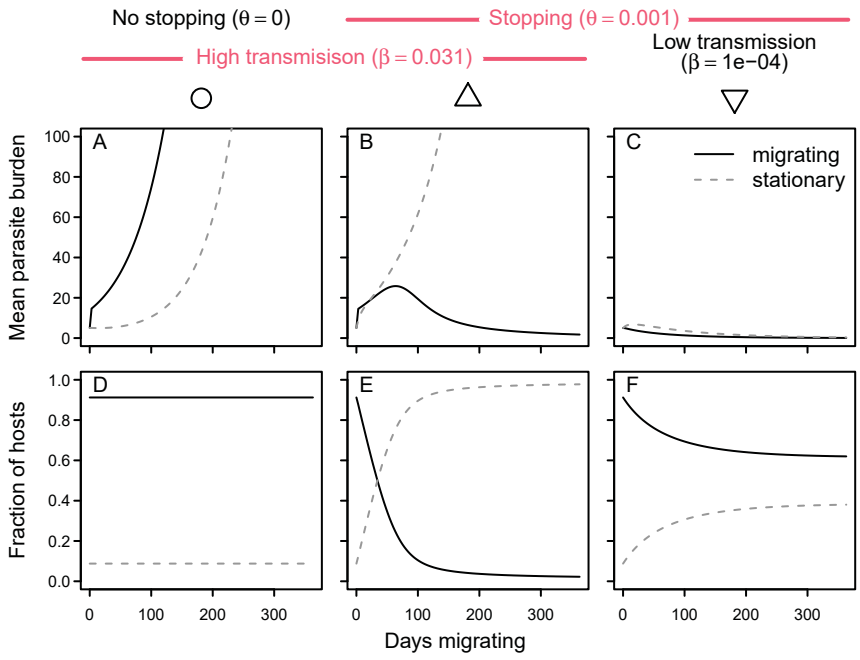
No stopping (θ = 0)
Stopping (θ = 0.001)
High transmisison (β = 0.031)
Low transmission
(β = 1e−04)
Mean parasite burden
Fraction of hosts
Days migrating
A
B
C
D
E
F
migrating
stationary
0
20
40
60
80
100
0.0
0.2
0.4
0.6
0.8
1.0
0
100
200
300